



# Several Microstrip-Based Conductor/Thin Film Ferroelectric Phase Shifter Designs Using $(\text{YBa}_2\text{Cu}_3\text{O}_{7-\delta}, \text{Au})/\text{SrTiO}_3/\text{LaAlO}_3$ Structures

F.W. Van Keuls, R.R. Romanofsky, and F.A. Miranda  
Lewis Research Center, Cleveland, Ohio

## The NASA STI Program Office . . . in Profile

Since its founding, NASA has been dedicated to the advancement of aeronautics and space science. The NASA Scientific and Technical Information (STI) Program Office plays a key part in helping NASA maintain this important role.

The NASA STI Program Office is operated by Langley Research Center, the Lead Center for NASA's scientific and technical information. The NASA STI Program Office provides access to the NASA STI Database, the largest collection of aeronautical and space science STI in the world. The Program Office is also NASA's institutional mechanism for disseminating the results of its research and development activities. These results are published by NASA in the NASA STI Report Series, which includes the following report types:

- **TECHNICAL PUBLICATION.** Reports of completed research or a major significant phase of research that present the results of NASA programs and include extensive data or theoretical analysis. Includes compilations of significant scientific and technical data and information deemed to be of continuing reference value. NASA's counterpart of peer-reviewed formal professional papers but has less stringent limitations on manuscript length and extent of graphic presentations.
- **TECHNICAL MEMORANDUM.** Scientific and technical findings that are preliminary or of specialized interest, e.g., quick release reports, working papers, and bibliographies that contain minimal annotation. Does not contain extensive analysis.
- **CONTRACTOR REPORT.** Scientific and technical findings by NASA-sponsored contractors and grantees.

- **CONFERENCE PUBLICATION.** Collected papers from scientific and technical conferences, symposia, seminars, or other meetings sponsored or cosponsored by NASA.
- **SPECIAL PUBLICATION.** Scientific, technical, or historical information from NASA programs, projects, and missions, often concerned with subjects having substantial public interest.
- **TECHNICAL TRANSLATION.** English-language translations of foreign scientific and technical material pertinent to NASA's mission.

Specialized services that complement the STI Program Office's diverse offerings include creating custom thesauri, building customized data bases, organizing and publishing research results . . . even providing videos.

For more information about the NASA STI Program Office, see the following:

- Access the NASA STI Program Home Page at <http://www.sti.nasa.gov>
- E-mail your question via the Internet to [help@sti.nasa.gov](mailto:help@sti.nasa.gov)
- Fax your question to the NASA Access Help Desk at (301) 621-0134
- Telephone the NASA Access Help Desk at (301) 621-0390
- Write to:  
NASA Access Help Desk  
NASA Center for AeroSpace Information  
800 Elkridge Landing Road  
Linthicum Heights, MD 21090-2934



# Several Microstrip-Based Conductor/Thin Film Ferroelectric Phase Shifter Designs Using $(\text{YBa}_2\text{Cu}_3\text{O}_{7-\delta}, \text{Au})/\text{SrTiO}_3/\text{LaAlO}_3$ Structures

F.W. Van Keuls, R.R. Romanofsky, and F.A. Miranda  
Lewis Research Center, Cleveland, Ohio

Prepared for the  
10th International Symposium on Integrated Ferroelectrics  
sponsored by the University of Colorado at Colorado Springs  
Monterey, California, March 1-4, 1998

National Aeronautics and  
Space Administration

Lewis Research Center

## Acknowledgments

We are grateful to C. Mueller and T. Rivkin for helpful discussions and technical support. We also thank S. Doyle (SCT), N. Varaljay, B. Viergutz, and E. McQuaid (LeRC) for fabricating the phase shifters.

Trade names or manufacturers' names are used in this report for identification only. This usage does not constitute an official endorsement, either expressed or implied, by the National Aeronautics and Space Administration.

Available from

NASA Center for Aerospace Information  
800 Elkridge Landing Road  
Linthicum Heights, MD 21090-2934  
Price Code: A03

National Technical Information Service  
5287 Port Royal Road  
Springfield, VA 22100  
Price Code: A03

SEVERAL MICROSTRIP-BASED CONDUCTOR/ THIN FILM  
FERROELECTRIC PHASE SHIFTER DESIGNS USING  
(YBa<sub>2</sub>Cu<sub>3</sub>O<sub>7-δ</sub>, Au)/SrTiO<sub>3</sub>/LaAlO<sub>3</sub> STRUCTURES

F. W. VAN KEULS,\* R. R. ROMANOFSKY, AND F. A. MIRANDA  
NASA Lewis Research Center, Cleveland, OH. 44135, U.S.A.

We have designed, fabricated, and tested several novel microstrip-based YBa<sub>2</sub>Cu<sub>3</sub>O<sub>7-δ</sub>/SrTiO<sub>3</sub>/LaAlO<sub>3</sub> (YBCO/STO/LAO) and Au/SrTiO<sub>3</sub>/LaAlO<sub>3</sub> (Au/STO/LAO) phase shifters. The first design consists of eight coupled microstrip phase shifters (CMPS) in series. This design using YBCO achieved a relative insertion phase shift ( $\Delta\phi$ ) of 484° with a figure of merit of 80°/dB at  $V_{dc} = 375$  V, 16 GHz, and 40 K. A  $\Delta\phi$  of 290° was observed while maintaining the insertion loss below 4.5 dB. At 77 K, a  $\Delta\phi$  of 420° was obtained for this phase shifter at the same bias and frequency. Both results correspond to an effective coupling length of 0.33 cm. A second compact design, consisting of an Au meander line and a CMPS section was also tested. Of the two samples tested, the best showed a figure of merit of 43°/dB with  $\Delta\phi = 290^\circ$  and 6.8 dB loss, at 40 K, 10 GHz and 400 V. Experimental and modeling results on these circuits will be discussed in the context of potential applications.

Keywords: microwave frequencies; phase shifter; ferroelectric thin films; microstrip lines; Ku-band; HTS thin films

## INTRODUCTION

Thin film ferroelectrics hold great promise for future microwave phase shifter technology. Light weight, compact, very low power, voltage tunable, planar phase shifters are realizable. However, it is still necessary to reduce microwave losses through ferroelectric material improvements and/or device design.

---

\*National Research Council—NASA Research Associate at Lewis Research Center

Several successful demonstrations of coplanar waveguide (CPW) HTS/ferroelectric phase shifters have been reported so far.<sup>[1,2]</sup> Nevertheless, for some applications, (for instance, in reflectarray antennas) the large ground planes of CPW are unsuitable because of specular reflections and other effects. In addition, different configurations may reduce the large microwave losses which are a major barrier to the use of this technology. With these considerations in mind, we have explored thin film ferroelectric phase shifters based on microstrip and coupled microstrip configurations. The vertical geometry of each of these designs is shown in Fig. 1. A single microstrip (Fig. 1(a)) can be tuned by applying a dc bias with respect to the ground plane. One might believe that very little tuning could be achieved because the capacitance between the line and ground changes little. However, with narrow microstrips, the relative dielectric constant ( $\epsilon_r$ ) of the STO is also tuned in areas adjacent to the microstrip, causing the effective dielectric constant ( $\epsilon_{\text{eff}}$ ) to change and hence shifting the insertion phase. We have measured this phase shift to be  $120^\circ$  on a 1 cm long  $50 \Omega$  YBCO microstrip line fabricated on  $2 \mu\text{m}$  STO/ $254 \mu\text{m}$  LAO at 40 K, 16 GHz and using 350 V dc bias. We will return to this configuration when discussing the meander line phase shifters.

The coupled microstrip geometry (Fig. 1(b)) can be excited in two modes: even and odd. The propagation constant is given by,

$$\beta = \omega / v_p = (\pi / \lambda_o) [(\epsilon_{\text{even}}(V_{\text{dc}}))^{0.5} + (\epsilon_{\text{odd}}(V_{\text{dc}}))^{0.5}] \quad (1)$$

where  $\lambda_o$  is the free space wavelength,  $v_p$  is the phase velocity,  $\epsilon_{\text{even}} = C_e / C_{e\text{-air}}$  and  $\epsilon_{\text{odd}} = C_o / C_{o\text{-air}}$ ;  $C_{e\text{-air}}$  and  $C_{o\text{-air}}$  are obtained by replacing all dielectrics with air. In the odd mode, the E fields are concentrated in the ferroelectric film. By applying a dc voltage between the two microstrips, the  $\epsilon_r$  of the ferroelectric between the lines can also be tuned with lower voltages than those required in Fig. 1(a). Hence, the coupled microstrip design can provide more phase shift per

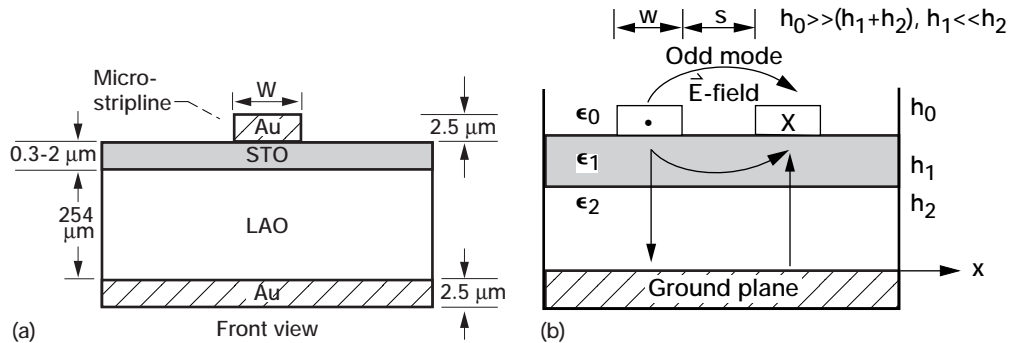


FIGURE 1 (a) The vertical configuration for a single microstripline on a thin STO film. (b) Coupled microstripline ferroelectric phase shifter schematic. The  $\vec{E}$  fields are drawn for odd mode propagation. For the  $50 \Omega$  CMPS,  $w = 25 \mu\text{m}$ ,  $s = 7.5 \mu\text{m}$ .

unit length at a given voltage than the simple microstrip. However, coupled micro-strip phase shifters (CMPS) require careful design because they are inherently filters with a limited bandwidth.

Figure 2 shows schematic representations of a  $25\ \Omega$  single-element CMPS (with input/output  $50\ \Omega$  to  $25\ \Omega$  transformers) and a  $50\ \Omega$  eight-element CMPS developed in this work.\* These phase shifters were modeled primarily using Sonnet's em<sup>®</sup> and to a lesser extent EEsof Touchstone<sup>®</sup> and Zeland's IE3D<sup>®</sup> electromagnetic simulators. An analytic model of a CMPS based in the quasi-TEM variational expressions of Koul and Bhat,<sup>[3]</sup> in combination with the transmission line method of Crampagne, *et al.*<sup>[4]</sup> was also developed to facilitate the design. The phase shifters were optimized to minimize microwave losses and maximize relative insertion phase shift.

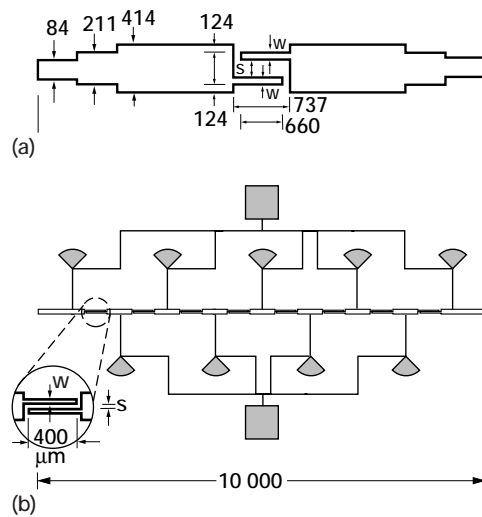


FIGURE 2 (a) Schematic of  $25\ \Omega$  single-element CMPS.  $S = 12.7\ \mu\text{m}$  and  $W = 76.2\ \mu\text{m}$ . All other dimensions are also in microns. (b) Schematic of eight-elements,  $50\ \Omega$  CMPS.  $S = 7.5\ \mu\text{m}$  and  $W = 25\ \mu\text{m}$ .

## EXPERIMENTAL

Strontium titanate was chosen as the ferroelectric film because, of those that we have tested (i.e. STO and BSTO), it has the best results in terms of tunability, maximum dielectric constant and low loss. A drawback is that STO can only be tuned advantageously at temperatures below 100 K. Both gold and  $\text{YBa}_2\text{Cu}_3\text{O}_{7-\delta}$  (YBCO) were used for the microstrip lines. Using YBCO reduces conductor loss and it can be grown epitaxially on the STO because of their close lattice match and chemical compatibility.

The films used in this study were purchased from SCT, Golden, CO. Below, we offer a brief description of their film deposition conditions. Deposition of the ferroelectric and HTS thin films was performed *in situ* on  $254\ \mu\text{m}$  thick, (100) single-crystal LAO substrates by laser ablation. The STO films were deposited at  $800\ \text{°C}$ , adjusting the deposition time so as to obtain films in the thickness

\*The  $25\ \Omega$  CMPS was designed to have lower conductor losses and was used more extensively because its larger gaps allowed for easier in-house fabrication by chemical etching.

range from 300 nm to 2.0  $\mu\text{m}$ . The film thickness was monitored by counting interference fringes using an ellipsometer.<sup>[5]</sup> This process was followed by the deposition of the YBCO films also at 800  $^{\circ}\text{C}$ . The typical thickness of the resulting YBCO films was 350 nm and their epitaxial nature was determined by x-ray diffraction analysis. Ion-milling and chemical etching were used for the YBCO devices. The fabrication of the Au circuits was performed at Lewis Research Center (LeRC). For the Au/STO/LAO phase shifters, Au films with nominal thickness of 2  $\mu\text{m}$  were deposited by electron beam evaporation on top of a 15 nm thick titanium adhesion layer e-beam evaporated before the metal deposition. Standard lift-off etching techniques were used to fabricate the Au structures.

The transmission ( $S_{21}$ ) and reflection ( $S_{11}$ ) scattering parameters of the CMPS were measured between 10 and 22 GHz, usually at 77 K and 40 K (near the peak  $\epsilon_r$  of STO), and at dc voltages up to 375 Volts, using an HP 8510C vector network analyzer and a closed-cycle helium gas refrigerator. For the single element CMPS, two bias tees were developed in-house to allow for dc bias through the SMA launchers up to 500 dc V and in the 10-22 GHz frequency range. Input and output terminals of the eight element CMPS were kept at dc ground. The latest version of this design uses thin Au lines of quarter-wavelength and radial stubs all connected by printed Au lines to two bias pads (see Fig. 2). All data were measured at a fixed temperature and frequency in a measurement cycle consisting of increasing the bias from zero to maximum bias, then decreasing the bias back to zero volts, changing polarity and increasing the bias to negative maximum bias, and lowering the voltage back to zero. The temperature stability was within  $\pm 0.1$  K during the measurement cycle.

## RESULTS

Figure 3 shows the phase shift of  $S_{21}$  versus dc bias for the single 25  $\Omega$  CMPS design using Au microstriplines with 350 nm, 1.0  $\mu\text{m}$ , and 2.0  $\mu\text{m}$  thick STO films. Also shown are data for a 300 nm thick YBCO/STO/LAO CMPS. Comparing the Au circuits, one can observe that the phase shift of this structure is nearly proportional to STO film thickness as predicted by quasi-TEM analysis. The experimental results obtained here are within a factor of two of the values for  $\Delta\phi$  ex-

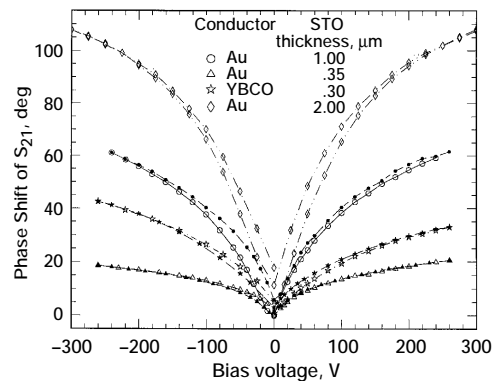


FIGURE 3 25  $\Omega$  coupled microstripline phase shifters;  $T = 77$  K, frequency = 13.73 GHz. Open (solid) symbols denote increasing (decreasing) bias.

pected from theoretical quasi-TEM predictions.<sup>[6]</sup> Figure 3 also shows that replacing the Au film by the YBCO film resulted in larger  $\Delta\phi$  values. While there is some variation in phase shift from sample to sample, the YBCO films generally showed larger phase shift. This may be due to a residual low  $\epsilon$  layer formed by the oxidized titanium adhesion film used in the gold circuit, or perhaps from an incompletely etched photoresist layer at the Au/Ti/STO interface. More study is required to account for this empirical behavior. The CMPS phase shifter also acts as a filter whose passband depends upon the STO film thickness and  $\epsilon_r$ . At high bias and low temperatures,  $\epsilon_r(\text{STO})$  reaches its smallest value and the passband its widest. As the bias voltage is lowered,  $\epsilon_r(\text{STO})$  increases and the CMPS' passband compresses. The data shown in Fig. 3 were taken at 77 K and 13.73 GHz, since this frequency remained within the passband as the bias was changed for all the different film thicknesses.<sup>[6]</sup>

In order to obtain larger phase shifts, we fabricated a phase shifter consisting of eight YBCO/STO/LAO CMPS in series (Fig. 2(b)). In the first iteration of this design, dc bias was applied to each element with a 25  $\mu\text{m}$  wide  $\lambda/4$  YBCO bias line attached to a radial stub which was individually wire-bonded to a bias pad. This bias network proved to be unreliable and lossy most probably because of adverse etching effects on the narrow YBCO bias lines and inaccurate placement of wire-bonds. The design was improved by using YBCO for the CMPS, but Au for the bias lines and radial stubs, and also by connecting the radial stubs together with printed Au lines. These changes improved reliability, phase shift and loss. The magnitude and phase shift of  $S_{21}$  for this circuit using a 1  $\mu\text{m}$  thick STO film are shown in Fig. 4 at 40 K and 77 K. The phase shift at 40 K is greater because the  $\epsilon_r$  of STO thin film is nearly maximum at this temperature, allowing for greater tuning. While  $\epsilon_r$  of bulk STO increases continuously with decreasing temperature, thin film STO exhibits a maximum  $\epsilon_r$  between 40 K and 80 K. Strain may be partially responsible for this difference, but the cur-

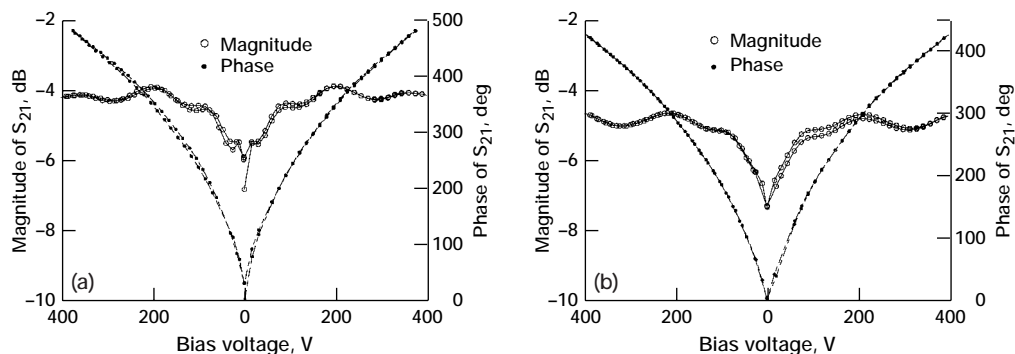


FIGURE 4 (a) 50  $\Omega$ , eight element CMPS using YBCO (.35  $\mu\text{m}$ )/STO (1.0  $\mu\text{m}$ )/LAO (254  $\mu\text{m}$ ). Data were taken at  $T = 40$  K and 16 GHz. (b) Same phase shifter as in (a). Data were taken at  $T = 77$  K and 16 GHz.

rently available evidence is inconclusive as to the cause. At 16 GHz, this device achieved a  $\Delta\phi$  of  $484^\circ$  while biasing  $V_{dc}$  from 0 to 375 V. If one restricts the bias range between 75 V and 375 V, a  $\Delta\phi$  of  $290^\circ$  was observed while maintaining the insertion loss below 4.5 dB. At 77 K (Fig. 4(b)), a  $\Delta\phi$  of  $420^\circ$  was obtained for this phase shifter at the same bias and frequency using to entire 375 V range. Both results correspond to an effective coupling length of 0.33 cm, with the microstrip mode in the  $50\ \Omega$  sections between the coupled fingers only contributing  $\sim 13^\circ$  of the total  $\Delta\phi$  in both cases.

Figure 5 shows the effect of bias on the passband of this device at 77 K. The zero bias curve has the narrowest and lowest frequency passband. Since  $\tan\delta$  of the STO also drops precipitously with bias,<sup>[7]</sup> this curve has much greater loss than the others. From 100 V to 400 V bias, the insertion loss does not change greatly but the passband shifts to a higher frequency. It is apparent why 16 GHz is the optimal operating frequency using 400 V. A lower frequency would have increased insertion loss at 400 V because of the passband edge. Alternatively, a lower frequency could be used if the bias were kept well below 400 V.

We also fabricated and tested phase shifters based primarily on a single microstrip line. This design, shown in Fig. 6, consists of a 3.7 cm long Au meander line and a single CMPS. The wider microstrip sections are intended to remove a resonance from our operating frequencies. We tested two samples with this circuit with STO film thicknesses of  $2\ \mu\text{m}$  and  $0.4\ \mu\text{m}$ . The insertion loss and phase shift for the  $2\ \mu\text{m}$  sample at 40 K and at 10 and 19 GHz are shown in Fig. 7(a). The Sonnet's em simulator results for 19 GHz are shown in Fig. 7(b). While the phase shift ( $\Delta\phi$ ) of  $690^\circ$  at 19 GHz is slightly lower than the simulations (assuming  $\epsilon_r(\text{STO})$  varies from  $\sim 500$  to 2500) the loss is very high ( $\sim 34\ \text{dB}$ ). The band-edge resonance occurs at a lower frequency than expected. At 10 GHz the losses are better but  $\Delta\phi$  is only  $360^\circ$ . The figure of merit at 10 GHz is  $30^\circ/\text{dB}$ . The results on the  $0.4\ \mu\text{m}$  sample, shown in Fig. 8, were more encouraging with a

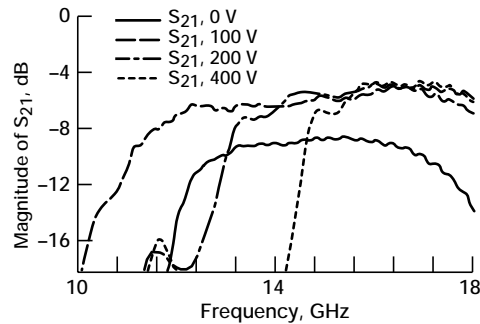


FIGURE 5 Frequency dependence of  $|S_{21}|$  for the eight-element,  $50\ \Omega$  CMPS using YBCO ( $.35\ \mu\text{m}$ )/STO ( $1.0\ \mu\text{m}$ )/LAO ( $254\ \mu\text{m}$ ) at 77 K.

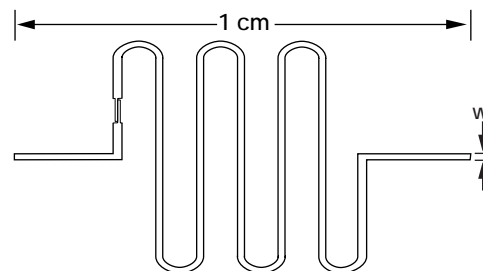


FIGURE 6 Meander line and 1 CMPS phase shifter. The linewidth  $w = 89\ \mu\text{m}$ .

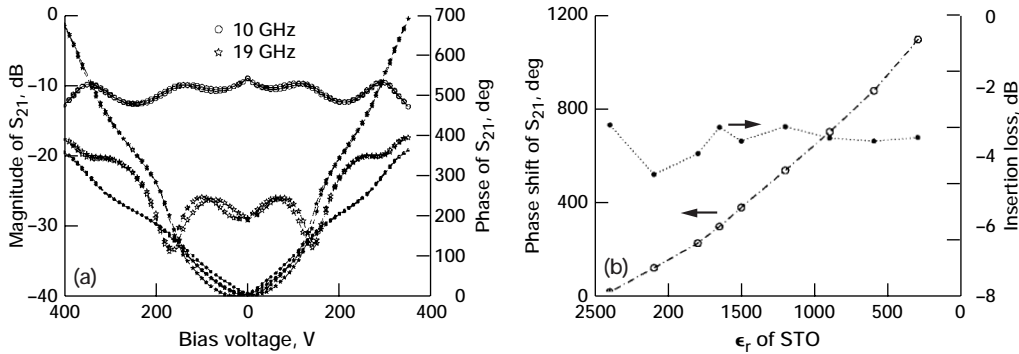


FIGURE 7 (a) The magnitude and phase shift of  $S_{21}$  vs. dc bias voltage for the meander line and one CMPS circuit using 2  $\mu\text{m}$  thick STO. The open symbols denote magnitude and the closed symbols denote phase shift. Data were taken at  $T = 40\text{ K}$ . (b) Sonnet em<sup>®</sup> simulation of insertion phase shift (left ordinate) and insertion loss (right ordinate) at 19 GHz for a meander line circuit on a 2  $\mu\text{m}$  thick STO film using  $\tan\delta_{\text{max}} = 0.008$ . The abscissa represents the dielectric constant of the STO film which decreases with increasing dc bias.

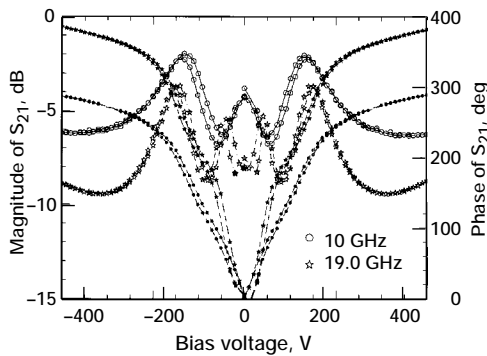


FIGURE 8 The magnitude and phase shift of  $S_{21}$  vs. dc bias voltage for the meander line and one CMPS circuit using 0.4  $\mu\text{m}$  thick STO. The open symbols denote magnitude and the closed symbols denote phase shift. Data were taken at  $T = 40\text{ K}$ .

higher figure of merit of  $43^\circ/\text{dB}$  with  $\Delta\phi = 290^\circ$  at 10 GHz.

The discrepancy between experiment and simulation could arise from higher than expected  $\tan\delta$  and/or lower  $\epsilon_r$ . It could also arise from a simplification inherent in the em simulation. The Sonnet\* and IE3D simulators assume that any given layer has a single  $\epsilon_r$ . While this assumption is true for modeling STO's change with temperature, the effects of bias lead to local variations in  $\epsilon_r$ . For instance, the biased region of STO around a microstripline does not extend very far. However, in a CMPS, the applied dc field extends between the two lines. This fact leads us to expect closer agreement between experiment and simulation in the CMPS than for a single microstrip. Further samples and design modifications of the meander line configuration will be tested.

Phased array antennas, particularly reflectarrays, will benefit from the phase shifter technology described herein. Conventional reflectarrays use interlaced spiral radiating elements interconnected with PIN diodes to provide perhaps 1.5 bits of phase resolution.<sup>[8]</sup> In this hybrid approach, the diode control circuitry

\*Sonnet's em simulator does have the capacity to do multiple  $\epsilon_r$ 's in a single layer but the process is so time and memory consuming as to limit its use only to small areas.

is cumbersome. Our ferroelectric phase shifters can be integrated with printed microstrip patch elements to enable a new type of reflectarray which can be produced lithographically. Since they will operate in a reflection mode, each must supply only  $180^\circ$  of phase shift. Their small cross section will minimize specular reflections from the front surface of the array, a feature unique to this implementation. For example, coplanar waveguide ferroelectric phase shifters require a fairly large ground plane on the same surface as the radiating element. Such phase shifters appear to be impractical for reflectarray applications because of this unwanted reflection. Recently demonstrated proof-of-concept thin film ferrite phase shifters<sup>[9]</sup> are also ill-suited for reflectarray applications because they require an induction coil to generate a magnetic field. This approach results in larger circuit size and awkward operation.

## CONCLUSIONS

In conclusion, we have presented data on several types of microstrip-based conductor/ferroelectric phase shifters. At 40 K and 16 GHz, the 8 element CMPS exhibited a figure of merit of  $80^\circ/\text{dB}$ . To our knowledge, these are the best results so far for phase shifters based on conductor/ferroelectric thin film technology and where miniaturization, insertion loss, and phase delay are key considerations. These results compare favorably with phase shifters based on similar technology reported by other researchers. For example, Gevorgian, *et al.*,<sup>[2]</sup> reported on a YBCO(300nm)/BSTO(900nm)/LAO coplanar waveguide (CPW) phase shifter with center conductor length  $\sim 0.4$  cm. For this component, they found a  $16^\circ/\text{dB}$  figure of merit at 50 K and 20 GHz. Our meander line and a single CMPS design exhibited a figure of merit of  $43^\circ/\text{dB}$  at 40 K and 10 GHz. These phase shifters are competitive with solid state switched-line phase shifters in terms of performance and size, and promise simplicity of fabrication and cost advantage. They show great promise for advantageous insertion in phased array systems particularly reflectarrays.

## Acknowledgments

We are grateful to C. Mueller (SCT) and T. Rivkin (SCT) for helpful discussions and technical support. We also thank S. Doyle (SCT), N. Varaljay (LeRC), B. Viergutz (LeRC), and E. McQuaid (LeRC) for fabricating the phase shifters.

## References

- [1.] A. T. Findikoglu, Q. X. Jia, and D. W. Reagor, *IEEE Trans. Appl. Supercond.*, **7**, 2925 (1997).
- [2.] S. S. Gevorgian, *et al.*, *IEEE Trans. Appl. Supercond.*, **7**, 2458 (1997).
- [3.] S. K. Koul and B. Bhat, *IEEE MTT-S Digest*, 489 (1981).
- [4.] R. Crampagne, M. Ahmadpanah, and J-L. Guiraud, *IEEE Trans. Microwave Theory Tech.*, **26**, 82 (1978).
- [5.] R. E. Treece, J. B. Thompson, C. H. Mueller, T. Rivkin, and M. W. Cromar, *IEEE Trans. Appl. Supercond.*, **7**, 2363 (1997).
- [6.] F. A. Miranda, R. R. Romanofsky, F. W. Van Keuls, C. H. Mueller, R. E. Treece, and T. V. Rivkin, *Integrated Ferroelectrics*, **17**, 231 (1997).
- [7.] M. J. Dalberth, R. E. Stauber, J. C. Price, C. T. Rogers, and D. Galt, *Applied Physics Letter*, **72**, 507 (1998).
- [8.] H.R. Phelan, *Microwave Journal*, **Dec.**, 41 (1976).
- [9.] D. E. Oates, G. F. Dionne, D. H. Temme, and J. A. Weiss, *IEEE Trans. Appl. Supercond.*, **7**, 2347 (1997).

# REPORT DOCUMENTATION PAGE

*Form Approved*  
*OMB No. 0704-0188*

Public reporting burden for this collection of information is estimated to average 1 hour per response, including the time for reviewing instructions, searching existing data sources, gathering and maintaining the data needed, and completing and reviewing the collection of information. Send comments regarding this burden estimate or any other aspect of this collection of information, including suggestions for reducing this burden, to Washington Headquarters Services, Directorate for Information Operations and Reports, 1215 Jefferson Davis Highway, Suite 1204, Arlington, VA 22202-4302, and to the Office of Management and Budget, Paperwork Reduction Project (0704-0188), Washington, DC 20503.

<b>1. AGENCY USE ONLY</b> ( <i>Leave blank</i> )	<b>2. REPORT DATE</b> May 1998	<b>3. REPORT TYPE AND DATES COVERED</b> Technical Memorandum	
<b>4. TITLE AND SUBTITLE</b> Several Microstrip-Based Conductor/ Thin Film Ferroelectric Phase Shifter Designs Using(YBa <sub>2</sub> Cu <sub>3</sub> O <sub>7-δ</sub> , Au)/SrTiO <sub>3</sub> /LaAlO <sub>3</sub> Structures		<b>5. FUNDING NUMBERS</b>  WU-632-50-5D-00	
<b>6. AUTHOR(S)</b>  F. W. Van Keuls, R. R. Romanofsky, and F. A. Miranda			
<b>7. PERFORMING ORGANIZATION NAME(S) AND ADDRESS(ES)</b>  National Aeronautics and Space Administration Lewis Research Center Cleveland, Ohio 44135-3191		<b>8. PERFORMING ORGANIZATION REPORT NUMBER</b>  E-11115	
<b>9. SPONSORING/MONITORING AGENCY NAME(S) AND ADDRESS(ES)</b>  National Aeronautics and Space Administration Washington, DC 20546-0001		<b>10. SPONSORING/MONITORING AGENCY REPORT NUMBER</b>  NASA TM-1998-206964	
<b>11. SUPPLEMENTARY NOTES</b>  Prepared for the 10th International Symposium on Integrated Ferroelectrics sponsored by the University of Colorado at Colorado Springs, Monterey, California, March 1-4, 1998. F.W. Van Keuls, National Research Council—NASA Research Associate at Lewis Research Center. R.R. Romanofsky, and F.A. Miranda, NASA Lewis Research Center. Responsible person, F.W. Van Keuls, organization code 5620, (216) 433-3379.			
<b>12a. DISTRIBUTION/AVAILABILITY STATEMENT</b>  Unclassified - Unlimited Subject Categories: 76 and 32  This publication is available from the NASA Center for AeroSpace Information, (301) 621-0390.		<b>12b. DISTRIBUTION CODE</b>	
<b>13. ABSTRACT</b> ( <i>Maximum 200 words</i> )  We have designed, fabricated, and tested several novel microstrip-base YBa <sub>2</sub> Cu <sub>3</sub> O <sub>7-δ</sub> /SrTiO <sub>3</sub> /LaAlO <sub>3</sub> (YBCO/STO/LAO) and Au/SrTiO <sub>3</sub> /LaAlO <sub>3</sub> (Au/STO/LAO) phase shifters. The first design consists of eight coupled microstrip phase shifters (CMPS) in series. This design using YBCO achieved a relative insertion phase shift ( $\Delta f$ ) of 484° with a figure of merit of 80°/dB at V <sub>dc</sub> = 375 V, 16 GHz, and 40 K. A $\Delta f$ of 290° was observed while maintaining the insertion loss below 4.5 dB. At 77 K, a $\Delta f$ of 420° was obtained for this phase shifter at the same bias and frequency. Both results correspond to an effective coupling length of 0.33 cm. A second compact design, consisting of an Au meander line and a CMPS section was also tested. Of the two samples tested, the best showed a figure of merit of 43°/dB with $\Delta f = 290^\circ$ and 6.8 dB loss, at 40 K, 10 GHz and 400 V. Experimental and modeling results on these circuits will be discussed in the context of potential applications.			
<b>14. SUBJECT TERMS</b>  Microwave frequencies; Phase shifter; Ferroelectric thin films; Microstrip lines; Ku-band; HTS thin films		<b>15. NUMBER OF PAGES</b> 15	
		<b>16. PRICE CODE</b> A03	
<b>17. SECURITY CLASSIFICATION OF REPORT</b> Unclassified	<b>18. SECURITY CLASSIFICATION OF THIS PAGE</b> Unclassified	<b>19. SECURITY CLASSIFICATION OF ABSTRACT</b> Unclassified	<b>20. LIMITATION OF ABSTRACT</b>